Contrib Mineral Petrol (1996) 124:111–125 

**G.P. Bulanova · W.L. Griffin · C.G. Ryan**
**O.Ye. Shestakova · S.-J. Barnes**

# Trace elements in sulfide inclusions from Yakutian diamonds

Received: 5 July 1995 / Accepted: 21 February 1996

**Abstract** Sulfide inclusions in diamonds may provide the only pristine samples of mantle sulfides, and they carry important information on the distribution and abundances of chalcophile elements in the deep lithosphere. Trace-element abundances were measured by proton microprobe in >50 sulfide inclusions (SDI) from Yakutian diamonds; about half of these were measured *in situ* in polished plates of diamonds, providing information on the spatial distribution of compositional variations. Many of the diamonds were identified as peridotitic or eclogitic from the nature of coexisting silicate or oxide inclusions. Known peridotitic diamonds contain SDIs with Ni contents of 22–36%, consistent with equilibration between olivine, monosulfide solid solution (MSS) and sulfide melt, whereas SDIs in eclogitic diamonds contain 0–12% Ni. A group of diamonds without silicate or oxide inclusions has SDIs with 11–18% Ni, and may be derived from pyroxenitic parageneses. Eclogitic SDIs have lower Ni, Cu and Te than peridotitic SDIs; the ranges of the two parageneses overlap for Se, As and Mo. The Mo and Se contents range up to 700 and 300 ppm, respectively; the highest levels are found in peridotitic diamonds. Among the *in-situ* SDIs, significant Zn and Pb levels are found in those connected by cracks to diamond surfaces, and these elements reflect interaction with kimberlitic melt. Significant levels of Ru (30–1300 ppm) and Rh (10–170 ppm) are found in many peridotitic SDIs; SDIs in one diamond with wustite and olivine inclusions and complex internal structures have high levels of other platinum-group elements (PGEs) as well, and high chondrite-normalized Ir/Pd. Comparison with experimental data on element partitioning between crystals of monosulfide solid solution (MSS) and sulfide melts suggests that most of the inclusions in both parageneses were trapped as MSS, while some high-Cu SDIs with high Pd±Rh may represent fractionated sulfide melts. Spatial variations of SDI composition within single diamonds are consistent with growth histories shown by cathodoluminescence images, in which several stages of growth and resorption have occurred within magmatic environments that evolved during diamond formation.

G.P. Bulanova[1]
Yakutian Institute of Geosciences, Lenin St. 39,
Yakutsk 677007, Russia

W.L. Griffin (✉) · C.G. Ryan
CSIRO Exploration and Mining, Box 136, North Ryde,
NSW 2113, Australia

W.L. Griffin
Key Centre for Geochemical Evolution and Metallogeny of
Continents, School of Earth Sciences, Macquarie University,
Sydney 2109, Australia

O.Ye. Shestakova
Kemerovsky Polytechnic Institute, 30 Leningradsky Avenue,
Kemerovo 650003, Russia

S.-J. Barnes
Sciences de la Terre, Universite due Quebec, Chicoutimi,
Canada, G7H 2B1

[1] *Present address:*
TsNIGRI, Varshavsky Ave. 129B, 119145 Moscow, Russia

Editorial responsibility: J. Touret

## Introduction

Inclusions in diamonds provide the most objective information about the chemical and physical environment in which diamonds grew. *Syngenetic* inclusions have been shielded by the diamond and protected from the surrounding environment since they were trapped. Knowledge of the major- and trace-element chemistry of these inclusions permits reconstruction of the conditions of diamond growth, and thus contributes to an understanding of the nature of processes in the upper mantle. *Epigenetic* inclusions may have formed after the diamond grew, or by modification of syngenetic inclusions exposed to the surrounding environment through cracks in the diamond crystal. They provide more ambiguous records of multistage processes, which may include the eruption of the host kimberlitic magma.

Sulfides in mantle-derived xenoliths and ophiolite massifs almost certainly have experienced recrystallization and reequilibration with silicates during and after their transport to the Earth's surface. Syngenetic sulfide inclusions in diamonds, on the other hand, have been shielded from interaction with the environment, provided the diamond has not cracked sufficiently to allow exchange between the inclusion and the surrounding environment. Analysis of sulfide inclusions in diamonds therefore can provide information on the primary compositions of mantle sulfides, and on the distribution and abundances of the chalcophile elements in the mantle. Both are directly relevant to understanding the genesis of magmatic sulfide deposits in gabbros, komatiites and ophiolites, and ultimately to an understanding of element fractionation in the early history of the Earth.

Iron-nickel-copper sulfides are the most widespread syngenetic inclusions in Yakutian diamonds (Bulanova et al. 1990) and in diamonds from African kimberlite pipes (Harris and Gurney 1979; Gurney et al. 1979). These sulfide inclusions (SDIs) are believed to have formed by the trapping of a primary liquid sulfide melt or crystals of monosulfide solid solution (MSS) during the growth of the diamond. Whereas the major-element compositions of SDIs have been studied extensively, trace-element data are scarce, due to the small size of the inclusions and the difficulty of extracting them from the diamonds. Erasmus et al. (1977) carried out NAA analyses of impurities in natural diamonds, and explained the presence of platinum-group elements (PGEs) in their data by the presence of microinclusions of sulfide minerals. Rudnick et al. (1992) presented ion-microprobe data on the S and Pb isotopic composition and Pb contents of some of the SDIs analyzed here, and Eldridge et al. (1991) gave similar data on African SDIs. McDonald et al. (1995) have carried out ICPMS (inductively coupled plasma-mass spectrometry) analysis of separated and dissolved inclusions from Orapa diamonds. There are some comparable data on trace-element compositions of sulfides in kimberlitic rocks; Rivers et al. (1990) and Paul et al. (1979) published trace-element analyses of sulfides in mantle-derived xenoliths from South African kimberlites. The trace-element compositions of sulfides in xenoliths from basalts, and in ophiolites, have been studied by Mitchell and Keays (1981), Page and Talkington (1984), Stockman and Hlava (1984), Page et al. (1986) and Lorand (1989).

We have used the proton microprobe to analyze the trace-element contents of >50 individual sulfide inclusions in Yakutian diamonds. Twenty-nine of these SDIs were analyzed *in situ* in polished plates of diamond; this approach allows each inclusion to be related to the growth pattern of the diamond (Bulanova 1995), and thus provides information on the evolution of sulfide composition with time. We also have analyzed inclusions that were extracted by crushing the diamonds; these data provide a broad background view of the variation in the contents of specific elements, relative to diamond paragenesis.

## Samples

The diamonds used in this study were recovered from the Mir and 23rd Party Congress kimberlite pipes (Malo-Botuobiya district) and the Udachnaya pipe (Daldyn district). These late Devonian kimberlites (Davis 1977) lie in the middle of the Siberian Platform.

Twenty-five inclusions were extracted by crushing diamonds from the Mir and Udachnaya pipes. For more detailed study of inclusions *in situ*, octahedral diamonds from all three pipes were sawn into plates parallel to the (110) plane, and the plates polished to expose the sulfide inclusions. The internal morphology and growth history of each diamond were revealed by studying these plates with UV photoluminescence, cathodoluminescence and polarized light (Bulanova in press). In the plates, it also was possible to check in detail for the presence of cracks connecting the inclusion to the surface of the diamond. Inclusions without such connecting cracks are considered to be syngenetic with the diamond growth zone in which they are located. Those with surface-connected cracks may be epigenetic, or at least altered by epigenetic processes. This is especially the case with SDIs near the rims of some diamonds. The syngenetic or epigenetic nature of the extracted inclusions is not known precisely.

Syngenetic inclusions are between 10 and 150 μm in diameter and typically have the shape of negative diamond crystals, which is consistent with their having grown synchronously with the diamond. There is no independent evidence regarding the temperature at which these sulfides were trapped in the diamonds studied here. However, Griffin et al. (1993) have used the Ni contents of chrome-pyrope inclusions, and the Zn contents of chromite inclusions, to measure trapping temperatures of 900–1400° C in other Siberian diamonds. In some of these diamonds, multiple inclusions show ranges of 200–400° C, and those diamonds were inferred to have grown during relatively short lived thermal events (Griffin et al. 1993). Other studies of in-situ inclusions of chromite and eclogitic minerals indicate that in general, temperatures decreased during the growth of the diamonds from core to rim (Bulanova in press). Most diamond-inclusion temperatures cluster between 900–1200° C (Griffin et al. 1992, 1993), and at these temperatures monosulfide solid solution (MSS) and sulfide melt coexist over a wide compositional range (Craig and Kullerud 1969; Leontievsky, personal communication).

The syngenetic SDIs therefore may have been trapped originally as sulfide melt, monosulfide solid solution (MSS) or pyrrhotite. In some of the lower-*T* diamonds, the MSS inclusions may have recrystallized during post-entrapment cooling. Most of the diamonds (and their SDIs) studied here probably were entrained in the kimberlite at ambient temperatures ≈900–1200° C, and may have been further heated in the ascending magma before being quenched by rapid eruption to the surface.

Petrographically, sulfide inclusions as now observed may consist of MSS, or of a fine-grained mixture of Fe−Ni−Cu−S phases exsolved from MSS during post-eruption cooling, according to the well-known phase relations of the Fe−Ni−Cu−S system (Craig and Kullerud 1969). The Ni-poor SDIs consist mainly of pyrrhotite with or without lamellae or thin rims of pentlandite; Ni-rich inclusions consist of Ni-rich MSS or of pentlandite with tiny inclusions of pyrrhotite. Chalcopyrite is rare, and may occur as a thin rim around pyrrhotite inclusions, or as small blocks and needles in the Fe−Ni sulfides. Observed multiphase intergrowths are very fine grained, and in general it seems unlikely that sectioning effects have seriously distorted observation of the relative abundances of the Cu−Fe−Ni phases. The large volumes (essentially entire inclusions; see below) analyzed by the proton microprobe also tend to average out these effects in terms of estimating the bulk composition of the original sulfides. However, some preferential sampling may be unavoidable, and the effects of this are considered below.

Diamonds can be divided into eclogitic and peridotitic parageneses, depending on the nature of their silicate inclusions, and the bulk compositions of SDIs in these two parageneses differ broadly in their Ni contents. Yefimova et al. (1983) suggested that peri-

dotitic SDIs contain >8% Ni, and eclogitic SDIs <8%. Two-phase inclusions of sulfide+comphacite and sulfide+coesite have been identified in eclogitic diamonds studied here, and the intergrowth of the sulfides with these typical syngenetic silicates further confirms the trapping of the sulfide during the growth of the diamond. Two sulfide inclusions from the central zone of one diamond (3648) were intergrown with wustite, and one coexisted with olivine ($Fo_{93}$); these are typical phases of the peridotitic paragenesis. Several inclusions located in the rims of diamonds, as well as some of the extracted ones, contain chalcopyrite+magnetite; these inclusions may be epigenetic.

## Analytical method

The inclusions were analyzed for Fe, Ni and trace elements using the HIAF proton microprobe at CSIRO Exploration and Mining, North Ryde. The instrument, analytical methods and data reduction have been decribed in detail by Ryan et al. (1990). The proton microprobe (PMP) is based on a tandem electrostatic accelerator, which provides a beam of 3 MeV protons. The proton beam is focused onto the sample by an electrostatic lens. In this work, the typical size of the beam spot on the sample was 30–50 microns, and beam currents were 7–12 nA. Samples were counted to a uniform accumulated live charge of 3 μC, corresponding to analysis times of 5–10 minutes. The characteristic X-rays generated by the proton bombardment are collected by a Si(Li) energy-dispersive detector and displayed as spectra. A 300 μm Al filter was placed between the sample and the detector to attenuate the Fe lines and thus reduce the overall count rate into the detector. Quantitative concentration data are extracted from the spectra as described by Ryan et al. (1990).

In most PMP analysis, normalization to known values for one element (for example, EMP data for Fe) is used to correct for differences in sample conductivity; otherwise the method is independent of external standards. In the present case, comparison with the EMP data was complicated by the heterogeneous nature of some inclusions. The proton beam analyzes to a depth of at least 30 μm; the volume sampled thus is considerably greater than that analyzed by the electron probe, and may include subsurface inclusions, e.g., of chalcopyrite or associated Ni-rich or Ni-poor phases. The analyses therefore were normalized to (FeS+NiS +CuS)=100%. This correction accounts for any overlap of beam onto the surrounding diamond or epoxy, but removes any possibility of calculating the stoichiometry of the original sulfides. To the extent that the stoichiometry deviates significantly from (Fe,Ni,-Cu)S, this normalization also introduces an equivalent percentage error in the Ni and Cu contents. In several cases, analyses are believed to be mixtures of Fe−Ni sulfide with wustite or magnetite; these are noted as such in the tables.

Typical analytical precision and accuracy are believed to be better than ±10% for most elements discussed here, with the reservation noted above with regard to stoichiometry. In the data tables, the concentration of each element is accompanied by estimates of precision (±1 SD) and minimum detection limit (MDL; 99% confidence limit).

## Results

The analytical data are presented in Table 1 and Figs. 1–4.

### Peridotitic and eclogitic parageneses

#### *Nickel*

There is a good overall agreement between the EMP and PMP data for Ni. In general, where significant differences occur, they are in the direction expected from minor mixtures of pyrrhotite and pentlandite; in low-Ni SDI the PMP Ni tends to be higher than the EMP values, while in the higher-Ni SDI the PMP Ni data tend to be lower. These differences are believed to be caused by the heterogeneous nature of some inclusions, coupled with

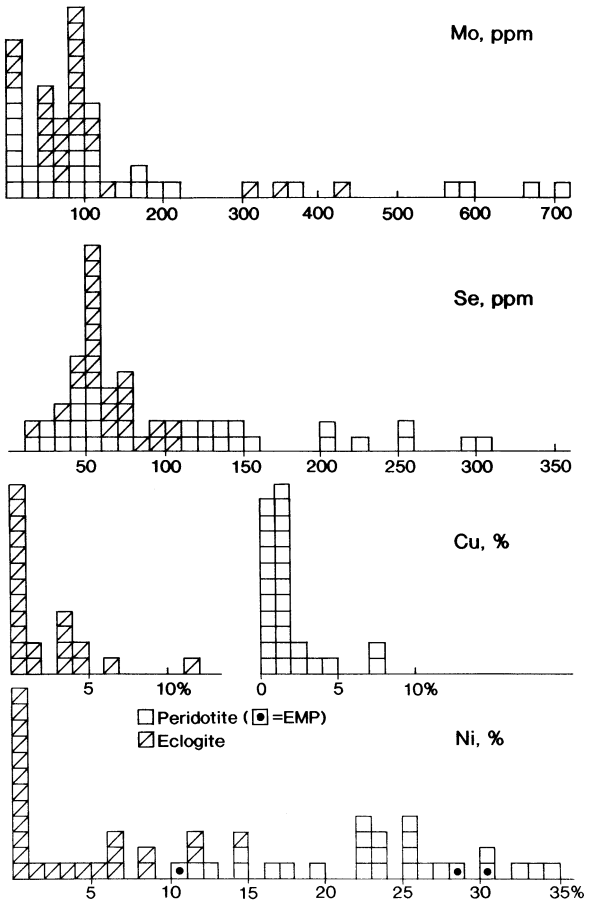


**Fig. 1** Histograms of element distribution in sulfide inclusions in diamonds

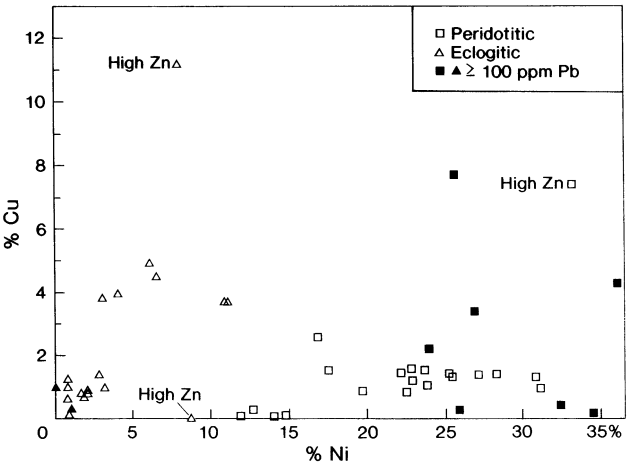


**Fig. 2** Cu versus Ni (PMP data unless otherwise noted) for sulfide inclusions

**Table 1** Peridotite sulphide inclusions in diamond (*Pn*) pentlandite, *Wus* wustite, *MSS* monosulphide solid solution, *Po* pyrrhotite, *Mgt* magnetite, *NF* not found, *NA* not analysed). Sample localities: nos. 1-1999, Mir pipe; 3000–3999, Udachnaya pipe; 4000–4999, 23rd Party Congress pipe; extracted inclusions, Mir and Udachnaya pipes

In-situ inclusions

| Sample | 3629 | 3629 | 3629 | 3648 | 3648 | 3648 | 3468 |
|---|---|---|---|---|---|---|---|
| Inclusion no. | 1.1 | 2.1 | 3.1 | 2.1 | 1.1 | 3.1 | 4.1 |
| Diamond zone | Core | Core | Core | Core | Core | Core | Inermediate |
| Diamond morphology | Octahedral | Octahedral | Octahedral | Cubo-octahedral | Cubo-octahedral | Cubo-octahedral | Octahedral |
| Luminescence color of zone | Blue | Blue | Blue | Blue | Blue | Blue | Blue |
| Observed phases | Pn | Pn | Pn | Pn | Pn+Wus | Pn+Wus | Pn |
| Coexisting phases, notes | | | Olivine[a] | ++[b] | | | |
| Crack to surface | No | No | No | No | No | No | No |
| %Fe (emp) | 33.4 | 35.4 | 36.3 | 38.3 | 43.8 | 41.3 | 38.1 |
| %Fe (pmp) | 31.7 | 37.2 | 38.9 | 46.0 | 47.9 | 39.5 | 37.4 |
| %Ni (pmp) | 31.2 | 25.3 | 23.8 | 16.5 | 14.5 | 22.8 | 25.1 |
| %Ni (emp) | 29.5 | 25.9 | 25.2 | 30.9 | 28.2 | 25.6 | 28.6 |
| %Cu (pmp) | 0.96 | 1.32 | 1.05 | 1.31 | 1.39 | 1.62 | 1.41 |
| Zn | <60 | <55 | <51 | NA | NA | NA | NA |
| As | <13 | <13 | <12 | NA | NA | NA | NA |
| Se | 254±14 | 299±16 | 301±16 | 45±6 | 43±7 | 58±6 | 45±4 |
| Mo | 10±2 | <8 | 8±2 | 590±17 | 571±19 | 679±17 | 704±23 |
| Te | <24 | 57±12 | 41±10 | <22 | <39 | 21±10 | 27±10 |
| Os | | | | 75±21 | 110±37 | 69±15 | 80±20 |
| Ir | | | | 92±17 | 153±21 | 170±20 | 99±15 |
| Ru | <9 | <9 | <9 | 233±13 | 195±13 | 311±15 | 90±5 |
| Rh | <10 | <10 | <9 | 23±4 | 28±7 | 28±4 | 10±3 |
| Pt | | | | <55 | <74 | <48 | <43 |
| Pd | 28±4 | 30±4 | 36±4 | 18±4 | <18 | 23±4 | <10 |
| Pb | <30 | <28 | <27 | <34 | <47 | <30 | <25 |

Extracted inclusions

| Sample | 3.1 | 4.5 | 5-4.1 | 5.5 | 5.1 | 9–4.1 | 9-6.1 |
|---|---|---|---|---|---|---|---|
| Observed phases | MSS | MSS | MSS | MSS | Pn | Po | Pn |
| %Fe (emp) | 27.5 | 26.1 | 36.1 | 40.5 | 35.3 | 47.7 | 27.5 |
| %Fe (pmp) | 29.8 | 23.9 | 38.9 | 40.0 | 31.4 | 48.0 | 29.4 |
| %Ni (pmp) | 26.7 | 36.2 | 23.6 | 22.8 | 32.3 | 12.7 | 34.4 |
| %Ni (emp) | 31.0 | 24.0 | 22.0 | 24.0 | 25.5 | 11.5 | 32.0 |
| %Cu (pmp) | 3.41 | 4.29 | 1.56 | 1.21 | 0.45 | 0.03 | 0.21 |
| Zn | 435±50 | 379±70 | <45 | <59 | 2400±250 | <39 | 1130±118 |
| As | <9 | 90±25 | <10 | 41±9 | 15±4 | <12 | <12 |
| Se | 144±7 | 250±30 | 208±12 | 34±4 | 53±4 | 73±7 | 113±7 |
| Mo | 26±2 | 100±13 | 88±5 | 154±24 | 9±2 | 32±3 | 11±2 |
| Te | 27±8 | 65±33 | 36±10 | <40 | <30 | <21 | <19 |
| Os | <97 | | <90 | <100 | <92 | | |
| Ir | <65 | | <64 | <73 | <61 | | |
| Ru | <8 | <24 | <8 | 1313±43 | <8 | <7 | <7 |
| Rh | <8 | <27 | <9 | 169±9 | <9 | <8 | <7 |
| Pt | <49 | | <55 | <55 | <48 | | |
| Pd | 18±4 | <29 | 50±5 | <12 | <9 | <8 | 13±3 |
| Pb | 130±10 | 880±71 | <23 | 34±14 | 119±12 | <27 | 1200±70 |

[a] Very small grain
[b] Intergrowth, mixed analysis

the much greater volume analyzed by the proton beam. However, the good agreement between EMP and PMP values for Ni in 31 of the 40 SDIs for which both analyses are available emphasizes the homogeneous nature of most inclusions on the scale of EMP and PMP analysis; it also suggests that deviations from FeS stoichiometry are generally small.

The Ni contents of the peridotitic SDIs fall into two main groups: 11–17.5% and 22–37%; the distribution in the latter is strongly skewed (Fig. 1), which may in part reflect error introduced by normalization of metal-deficient MSS to FeS stoichiometry. In constructing this figure, the EMP data have been used for two analyses (3648/6-2.1, 6-1.1) where mixture with olivine or

**Table 1** (continued)

| 3648 | 3648 | 3648 | 3648 | 3648 | 2016 |
|---|---|---|---|---|---|
| 1.1 | 2.1 | 3.1 | 8 | 9 | 3 |
| Peripheral | Peripheral | Peripheral | Peripheral | Peripheral | Peripheral |
| Octahedral | Octahedral | Octahedral | Octahedral | Octahedral | Octahedral |
| Blue | Blue | Blue | Blue | Blue | Blue |
| Pn | Pn | Pn | Pn+Mgt | Pn | Pn |
| Yes | Yes | Yes | Yes | No | No |
| 42.4 | 29.9 | 35.7 | 56.5 | NA | 40.0 |
| 44.8 | 26.2 | 35.7 | 58.0 | 34.9 | 43.3 |
| 17.5 | 25.4 | 25.7 | 5.3 | 23.8 | 19.4 |
| 22.2 | 25.7 | 31.2 | 10.0 | | 21.5 |
| 1.54 | 7.72 | 0.28 | 0.4 | 2.27 | 1.26 |
| NA | NA | NA | NA | 3.74% | <40 |
| NA | NA | NA | NA | <15 | NA |
| 65±6 | 58±7 | 49±9 | 25±4 | 53±17 | 205±12 |
| 180±6 | 163±6 | 111±5 | 370±8 | 114±4 | 173±9 |
| 27±8 | <24 | <23 | 19±6 | <19 | 29±10 |
| <45 | <52 | 59±20 | 44±16 | <119 | <70 |
| 99±22 | <121 | <81 | <40 | <83 | <51 |
| 38±4 | 53±4 | 133±8 | 123±5 | 41±3 | 55±5 |
| <9 | <10 | <11 | 13±2 | <7 | 8±3 |
| <49 | <86 | <61 | <33 | <58 | <39 |
| 9±3 | 12±4 | <12 | <7 | 7±2 | 31±5 |
| 62±9 | 342±27 | 208±16 | <22 | 238±18 | <24 |

| 9-9.1 | 9-13.1 | 9-14.1 | 9-16.1 | 10-1.1 | 10-20.1 | 10-6.1 | 10.12 | 10-3.5 |
|---|---|---|---|---|---|---|---|---|
| MSS | Pn | Pn | MSS | MSS | Pn | Po | MSS | Po |
| 49.6 | 42.5 | 26.8 | 44.0 | NA | NA | NA | NA | NA |
| 40.6 | 40.4 | 23.8 | 44.6 | 20.3 | 35.6 | 51.8 | 49.7 | 48.9 |
| 22.5 | 22.1 | 33.2 | 16.8 | 43.8 | 27.1 | 11.8 | 14.0 | 14.9 |
| 14.0 | 15.9 | 36.4 | 19.0 | 43.0 | 25.0 | NA | NA | NA |
| 0.86 | 1.44 | 7.38 | 2.54 | 0.14 | 1.36 | 0.06 | 0.06 | 0.03 |
| <75 | <77 | 260±69 | <59 | <45 | <64 | | 188±36 | <42 |
| <17 | <17 | <18 | <14 | <10 | <14 | | <22 | <13 |
| 17±4 | 29±4 | 121±9 | 128±8 | 32±3 | 145±9 | 138±9 | 153±18 | 223±13 |
| 62±5 | 96±6 | 13±4 | 44±5 | 80±5 | 210±10 | 86±5 | 52±5 | 16±2 |
| <24 | <28 | <27 | <30 | <16 | 28±10 | 23±9 | <27 | <25 |
| | | | <98 | | | <50 | | |
| | | | <67 | | | <55 | | |
| 13±3 | <11 | 16±5 | 86±7 | <7 | 9±3 | 60±7 | 60±6 | <8 |
| <11 | <10 | <12 | <12 | <7 | <10 | <9 | 14±4 | <7 |
| | | | <51 | | | <47 | | |
| <12 | 18±4 | 17±4 | 19±5 | <7 | <11 | <10 | <12 | 17±3 |
| <38 | <38 | <33 | <31 | <22 | <32 | <31 | <48 | <28 |

wustite is suspected in the PMP data, and for one low-Ni inclusion from the same diamond (3648/8) which is suspected of having suffered secondary alteration. One inclusion is an outlier, with ≈44% Ni. About half of the eclogitic SDIs contain ≤1% Ni; there is a nearly continuous range up to >11% Ni, which overlaps the Ni contents of the peridotitic suite. Two of these high-Ni inclusions occur in a diamond (4173) that also contains omphacite and coesite inclusions and therefore is definitely identified as eclogitic. These data suggest that a 12% Ni boundary between eclogitic and peridotitic sulfides may be more appropriate than the 8% Ni value used by Yefimova et al. (1983), but this boundary probably is transitional rather than sharp. It also is possible that a third, pyroxenitic paragenesis is represented: this will be discussed below.

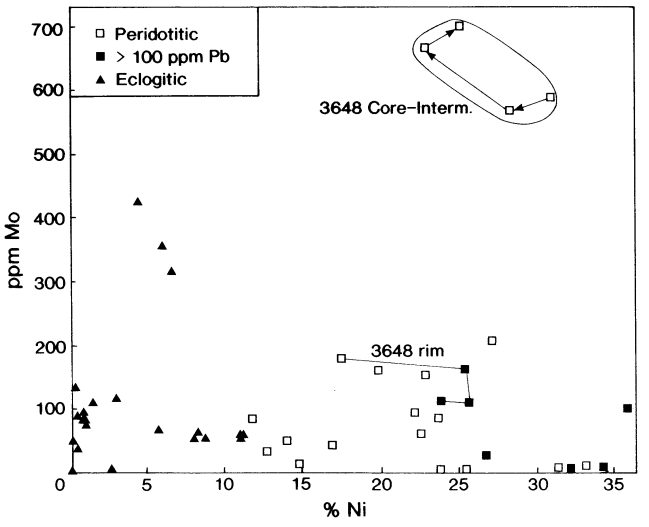


**Fig. 3** Mo versus Ni (PMP data unless otherwise noted) for sulfide inclusions

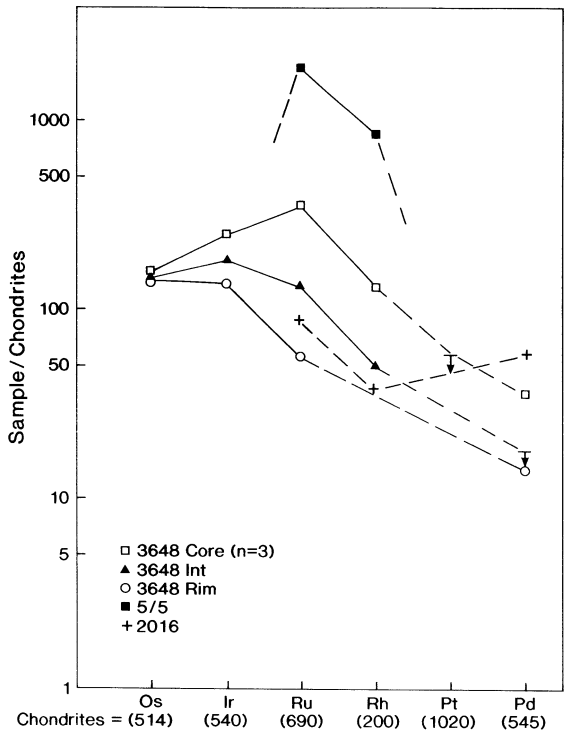


**Fig. 4** Chondrite-normalized PGE patterns in diamonds from different growth zones of diamond 3648 (see Fig. 5), and inclusion 5/5. *Arrows* show MDL for Pt (all samples) and Pd (3648-Int.); see also Table 1

### *Copper*

Seventy five percent of the peridotitic SDIs contain <2% Cu, and there is no correlation between Cu and Ni contents. Over half of the eclogitic SDIs contain <1% Cu, but there is a significant group with 3–5% Cu, all of which also are in the higher-Ni group noted above. Within the eclogitic SDIs there is an overall positive correlation between Ni and Cu (Fig. 2). This is regarded as a primary feature, because sampling effects on pyrrhotite-pentlandite-chalcopyrite mixtures would produce a negative correlation.

### *Zinc, cadmium, lead*

Zinc generally is below detection (ca. 30 ppm) in the *in-situ* inclusions of the peridotitic group; the exceptions are several in outer zones, where interaction with the surrounding environment may have occurred. High values of Zn (>300 ppm) typically are associated with high Pb contents (>100 ppm). Among the *in-situ* SDIs, Pb contents >50 ppm are found mainly in those near the rims of diamonds, and/or associated with fractures connected to the surface (Tables 1, 2). These high Pb contents (and by analogy the high Zn contents) therefore are regarded as the result of contamination with material from the surrounding kimberlite. Zinc is present at levels of 25–200 ppm in several of the eclogitic SDIs, without accompanying high levels of Pb. Mantle olivine typically contains ≈55 ppm Zn (Ryan et al. 1996) and eclogitic garnet and pyroxene commonly contain 50–150 ppm Zn (O'Reilly and Griffin 1995). The low values of Zn in most SDIs therefore are consistent with $D_{Zn}^{sulfide/silicate}$ values of <1–2, and suggest that Zn behaves primarily as a lithophile element in the mantle environments where diamond formed. Cadmium was detected in several inclusions with percent levels of Zn; the Zn/Cd ratio ranges from 90–250.

### *Selenium*

Selenium is present in all inclusions analyzed. In the eclogitic SDIs it ranges from 16–106 ppm, with a pronounced peak at about 50 ppm (Fig. 1); Pactunc et al. (1990) report a similar range of 10–200 ppm in pyrrhotite from magmatic sulfide deposits. In the peridotitic SDIs Se ranges from 17–300 ppm, with one pronounced peak near 50 ppm (as in the eclogitic SDIs) and another from 110–160 ppm. The highest Se contents (255–300 ppm) are found in sulfides from the central zone of peridotitic diamond 3629. The ranges seen here are similar to those reported in sulfides from mantle-derived xenoliths in kimberlites (Rivers et al. 1990). Pactunc et al. (1990) report an even larger range (<10–>900 ppm) in pentlandite from magmatic sulfide deposits.

### *Arsenic*

Arsenic is below detection in all of the eclogitic SDIs; this contrasts with the concentrations of up to 1% found in sulfides from eclogitic xenoliths (Rivers et al. 1990). In the peridotitic SDI, As was not found in the *in-situ*

SDIs, but significant values were found in three of the extracted inclusions, some of which may be epigenetic, judging from their high Zn and/or Pb contents (see above). Arsenic levels of 0.1–1 ppm have been reported in Norilsk ores (Zientek et al. 1994).

*Tellurium*

Tellurium contents are below detection ($\approx$25 ppm) in all but three of the eclogitic SDIs, but range from 20–65 ppm in many of the peridotitic SDIs. Pactunc et al. (1990) reported a few pyrrhotites with 10–30 ppm, and a few pentlandites with 20–80 ppm Te, while most of the sulfides they analyzed did not contain detectable Te. The MSS in Norilsk ores contains ca 1 ppm Te, rising to 20 ppm in Cu-rich ores (Zientek et al. 1994). The levels of Te in mantle and crustal sulfides therefore may be comparable.

*Molybdenum*

In the eclogitic SDIs Mo ranges from 50–424 ppm, with most values between 50–100 ppm and a median of $\approx$80 ppm (Fig. 1). The range is greater in the peridotitic SDIs, with values up to 700 ppm, but the median value for this group also is $\approx$80 ppm. The highest values are found in the core-zone SDIs of diamond 3648; if this one stone is excluded, the mean Mo value of peridotitic SDIs drops from 160 ppm to 58 ppm. Those SDIs with Ni>30% generally have very low Mo contents. In the interior parts of diamond 3648 there is a good correlation between Mo contents and the Ni contents determined by the proton microprobe (Fig. 3), but not between Mo (PMP) and Ni from the electron probe. This discrepancy is believed to reflect the larger volume (essentially the whole inclusion) analyzed by the proton probe. The Ni-Mo variations seen in the PMP data for diamond 3648 therefore may show the relations in the sulfide originally trapped in the diamond. Rivers et al. (1990) have reported Mo values up to 50 ppm in sulfides from Roberts Victor eclogite xenoliths, augite megacrysts and a veined lherzolite xenolith from Bultfontein Mine.

*Platinum group elements (PGE)*

All of the PGEs are below detection in all of the eclogitic SDIs. However, a range of PGEs is present at levels of tens to hundreds of ppm in some peridotitic SDIs. Pentlandite typically can take up significant levels of Pd; Pactunc et al. (1990) report many values in the range 100–300 ppm, with some up to >550 ppm, while Li et al. (1993) report an average of 1.7 ppm Pd in pentlandite from the Sudbury ores. If the observed variation in PGE contents were a sectioning effect reflecting different pentlandite/pyrrhotite ratios in the analyzed volumes, a positive correlation between Ni and Pd might be expected. This is not observed in the data in Table 1.

In diamond 3648 Os, Ir, Ru,Rh and Pd are present at levels 10–400× chondrites in several inclusions, in both core and rim, but Pt is below detection in all. The SDIs from the core of the crystal show a chondrite-normalized PGE pattern that is enriched in Os, Ir and Ru relative to Pd. The inclusions from the outer part of the crystal have lower total PGE levels, and a smoother PGE pattern, with Rh and Pd progressively depleted relative to Os and Ir. Copper and Ni remain essentially constant through the core and intermediate zones, but vary irregularly in the peripheral zone.

The *in-situ* inclusion in diamond 2016 has relatively high Pd and Ru contents, with Rh near the MDL (Fig. 4). The extracted inclusion 5/5 has even higher Ru and Rh contents, but the other PGEs are below detection. Several other inclusions also show measurable levels of Ru$\pm$Rh but not of the other PGEs. A third class is represented by inclusions such as 5/4 and 9/14, which contain low but significant Pd$\pm$Ru, although none of the other PGEs are above detection.

The Ir/Pd ratios of the SDIs from diamond 3648 range from 5–11. These ratios are markedly higher than those of most mantle-derived garnet peridotite xenoliths. However, similar values are found in spinel lherzolite xenoliths and alpine peridotites; the closest analogues to the SDI patterns are found in the chromitite layers of alpine peridotite complexes. The humped Ru-Rh-enriched pattern of inclusions 5/5 is similar to that shown by some sulfides from komatiites and from the marginal zones of the Bushveld intrusions, which are enriched in Ru and Rh but depleted in Os, Ir and Pt. However, all of these samples also show enrichment in Pd, which is not observed in the SDIs.

The PGE patterns of these SDIs are quite different from those of kimberlites (McDonald et al. 1995; Kaminsky et al. 1974), ruling out an origin by contamination from this source. The absolute values of PGEs, especially Os, Ir and Ru, in these sulfides are very high, exceeding those of the most enriched magmatic sulfide deposits by nearly 10×. The highest PGE levels in diamond 3648 are found in SDIs in the core of the stone, and the low Pb and Zn contents of these inclusions argue against the influence of any secondary processes. The high PGE levels and their variations across diamond 3648 therefore are regarded as primary features.

Spatial variation within single diamonds

Several of the diamonds studied here contain >1 inclusion, allowing us to study the variation of sulfide chemistry with time, during growth of the enclosing diamond. The internal structure of the diamonds, and hence the relative position of the inclusions in the growth history, can be revealed by images of UV photoluminescence or cathodoluminescence.

**Table 2** Compositions of eclogite-paragenesis sulphides. (Abbreviations as for Table 1 and, *Ccp* chalcopyrite, *Coes* coesite, *cpx* omphacite). Sample localities: 1153–1607, Mir pipe; 4173, 23rd Party Congress pipe; extracted inclusions, Mir and Udachnaya

In-situ inclusions

| Sample | 1153 | 1153 | 1153 | 1584 | 1591 | 1594 | 1594 |
|---|---|---|---|---|---|---|---|
| Inclusion no. | 2.1 | 1.1 | 1 | 1 | 1 | 4 | 5 |
| Diamond zone | Intermediate | Intermediate | Peripheral | Intermediate | Peripheral | Peripheral | Peripheral |
| Morphology of zone | Rounded | Rounded | Octahedral | Octahedral | Octahedral | Octahedral | Octahedral |
| Luminescence color of zone | Yellow | Yellow | Blue | Blue | Blue | Blue | Blue |
| Observed phases | Po | Po | Po | Po | Po+Mgt | Po+Mgt | Ccp*Mgt |
| Coexisting phases, notes | | | | Coes+Cpx | | | [a] |
| Fe (emp) | 48.3 | 51.5 | 53.0 | 51.3 | 55.9 | 58.4 | 60.3 |
| %Fe (pmp) | 53.0 | 55.5 | 56.9 | 52.6 | 59.5 | 61.9 | 62.5 |
| %Ni (pmp) | 6.04 | 4.4 | 3.00 | 6.70 | 2.73 | 0.96 | 0.08 |
| %Ni (emp) | 2.75 | 5.01 | 4.84 | 6.70 | 2.79 | 0.97 | 0.39 |
| %Cu (pmp) | 4.86 | 3.92 | 3.86 | 4.5 | 1.42 | 0.74 | 0.98 |
| Zn | <90 | 120±63 | 197±81 | 127±24 | <39 | <33 | 25±12 |
| As | <19 | <15 | <23 | <15 | <11 | <11 | <8 |
| Se | 60±6 | 56±5 | 45±8 | 50±6 | 97±6 | 53±4 | 52±4 |
| Mo | 354±18 | 424±21 | 117±8 | 318±11 | <8 | 86±4 | 56±3 |
| Te | <42 | <24 | <55 | <27 | <23 | <20 | <14 |
| Ru | <16 | <10 | <15 | <11 | <8 | <7 | <5 |
| Rh | <18 | <10 | <16 | <10 | <8 | <7 | <5 |
| Pb | <43 | <33 | <52 | <35 | <24 | <24 | 202±14 |

Extracted inclusions

| Sample | 10.8.1 | 10.15 | 10.16 | 9.3 | 9.7.1 | 9.8.1 | 9.10.1 |
|---|---|---|---|---|---|---|---|
| Inclusion no. | 8.1 | 15 | 16 | 3 | 7.1 | 8.1 | 10.1 |
| Assemblage | Ccp | Po | Po | Po | Po | Po+Ccp | Po |
| %Fe (emp) | NA | NA | NA | 62.8 | 62.0 | 24.8 | 50.0 |
| %Fe (pmp) | 26.0 | 61.1 | 62.7 | 63.0 | 62.3 | 20.6 | 55.5 |
| %Ni (pmp) | 0 | 1.56 | 0.45 | 0.41 | 0.3 | 8.06 | 8.18 |
| %Ni (emp) | 0 | 1.56 | 0.44 | 0.44 | 0.4 | 8.72 | 8.18 |
| %Cu (pmp) | 39.3 | 0.94 | 0.37 | 0.08 | 0.96 | 36.7 | 0.04 |
| Zn | 1075±200 | 55±21 | <37 | 35±8 | 3780±380 | 3.10% | 285±41 |
| As | <10 | <13 | <13 | <11 | <11 | <25 | <25 |
| Se | 73±3 | 106±7 | 55±6 | 51±4 | 71±5 | 78±17 | <16 |
| Mo | <7 | 110±5 | 90±5 | 91±4 | 134±5 | 53±10 | 62±10 |
| Te | <20 | <26 | <25 | <21 | <21 | <124 | <43 |
| Ru | <7 | <8 | <9 | <8 | <7 | <29 | <16 |
| Rh | <7 | <8 | <9 | <8 | <7 | <30 | <17 |
| Pb | 31±5 | <30 | <30 | <24 | 115±9 | 796±56 | 74±14 |

[a] Intergrowth, mixed analysis?
[b] Crack to surface

*Diamond 3648 (peridotitic paragenesis)*

This stone has the most complicated internal morphology and the most unusual sulfide geochemistry of those examined here. The cathodoluminescence image of the central plate from this diamond shows that it consists of three areas (Fig. 5). The central area is cubo-octahedral and luminesces blue; this zone contains three sulfide inclusions (6-1.1, 6-2.1, 6-3.1), wustite and a small inclusion of olivine ($Fo_{93}$). The intermediate part of the crystal is octahedral, and the truncation of the zoning pattern shows evidence of intensive non-uniform resorption of two parallel faces of the octahedron. This is especially clear on two sides, on one of which another inclusion of pentlandite (7-3.1) is located. This picture of selective resorption in the intermediate zone is not common; nor-

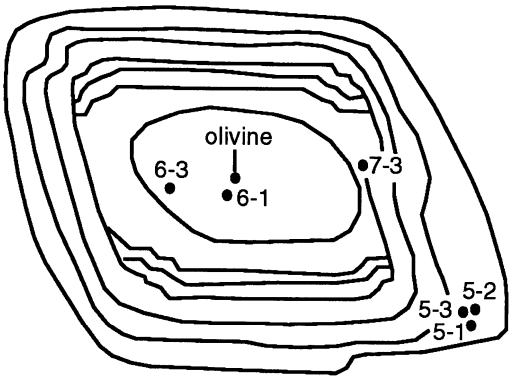


**Fig. 5** Sketch of cathodoluminescence image of diamond plate 3648, showing growth zones, resorption features, and location of SDIs. Width of crystal 4.2 mm

**Table 2** (continued)

| 1607 | 1607 | 1607 | 1607 | 1607 | 1607 | 1607 | 4173 | 4173 |
|---|---|---|---|---|---|---|---|---|
| 1.2 | 2.1 | 2.2 | 3.1 | 3.2 | 4.1 | 4.2 | 1.1 | 2.1 |
| Core | Core | Intermediate | Intermediate | Intermediate | Peripheral | Pheripheral | Intermediate | Peripheral |
| Octahedral | Octahedral | Octahedral | Octahedral | Octahedral | Octahedral | Octahedral | Octahedral | Octahedral |
| Blue | Yellow | Blue | Blue | Blue | Blue | Blue | Blue | Blue |
| Po | Po | Po | Po+Ccp Cpx | Po | Po | Po [b] | Po Coes+Cpx | Po |
| 59.0 | 59.3 | 58.4 | NA | 59.3 | 58.8 | 48.0 | NA | NA |
| 62.0 | 61.8 | 61.4 | 21.8 | 62.0 | 62.0 | 49.1 | 49.0 | 49.0 |
| 0.85 | 0.98 | 0.82 | 8.7 | 0.74 | 0.83 | 14.3 | 11.2 | 11.1 |
| 1.14 | NA | NA | 1.83 | NA | 1.06 | NA | 9.37 | 9.19 |
| 0.68 | 0.87 | 1.29 | 35.7 | 0.8 | 0.72 | 0.45 | 3.69 | 3.75 |
| 79±15 | <58 | 94±42 | 3.16% | 53±18 | <38 | 166±38 | 69±18 | 304±68 |
| <12 | <17 | NA | <41 | NA | <12 | NA | <14 | <24 |
| 59±4 | 56±5 | 72±6 | 82±18 | 60±6 | 69±5 | 24±7 | 95±7 | 106±1 |
| 86±5 | 79±5 | 88±5 | 55±11 | 82±5 | 94±4 | 45±7 | 60±4 | 57±6 |
| 21±8 | <26 | <21 | <130 | <24 | <22 | <53 | <22 | <62 |
| <8 | <9 | <7 | <30 | <8 | <8 | <15 | <9 | <17 |
| <9 | <10 | <7 | <32 | <8 | <9 | <17 | <10 | <18 |
| <27 | <37 | <22 | 808±60 | 38±12 | <27 | 135±28 | <31 | <53 |

| 9.15.1 | 9.2 |
|---|---|
| 15.1 | 20.1 |
| Po | Po |
| 57.3 | 50.5 |
| 61.7 | 51.3 |
| 0.81 | 5.72 |
| 0.61 | 9.1 |
| 11.1 | 6.90 |
| 49±15 | 101±30 |
| <15 | <15 |
| 52±5 | 52±6 |
| 91±8 | 68±4 |
| <24 | <27 |
| <9 | <10 |
| <9 | <10 |
| <41 | <34 |

mally the points and edges of the octahedron being to resorb first. This may indicate either some non-isometric fluid flow pattern, or that the crystal was broken on two sides of the octahedron before the resorption.

The outer or peripheral area of the crystal consists of several thin zones, which also show signs of dissolution, especially at the points of the octahedron. Five inclusions of sulfides occurred in this zone, some of which (5-1.1 to 5-3.1, 8) showed cracks leading to the surface of the diamond. This is consistent with the high Pb contents of inclusions 5-1.1 to 5-3.1; however, inclusion 9 had no obvious cracks connecting it to the surface, but still has high Pb. A recent detailed cathodoluminescence study of this diamond by Taylor et al. (1995) suggests that the diamond has undergone several episodes of brittle fracture and regrowth, especially in the outer part, and that the SDIs in the outer part lie on healed fractures. This fracturing may therefore have allowed partial reequilibration of the sulfides with fluids from the surrounding environment.

The compositions of the SDIs in the outer rim are widely variable, and this may reflect different degrees of interaction between the sulfide inclusion and the surrounding medium. In general, the Mo contents of the SDIs increase from the core to the intermediate zone, and then decrease sharply to the rim (Fig. 3), whereas the overall PGE contents of the SDIs decrease steadily from core to rim (Fig. 3). There is a clear fractionation of the PGE relative to one another from core to rim, with the Ir/Rh ratio increasing as the total PGE contents decrease (Fig. 4).

*Diamond 1153 (eclogitic paragenesis)*

The cathodoluminescence image of this diamond shows three main stages of growth (Fig. 6). The very small central area of the stone is cubic and shows bright yellow luminescence. The intermediate zone has a rounded shape and a weak yellow luminescence, while the outer part consists of three octahedral zones with blue luminescence. Two sulfides from the intermediate zone and one from the outer part have been analyzed. The main difference in composition is in Mo, which drops from 350–430 ppm in the intermediate zone SDIs to 117 ppm in the outer zone.

*Diamond 1607 (eclogitic paragenesis)*

This octahedral diamond shows no change in morphology during growth. The central area luminesces yellow, while the other zones luminesce blue. In the intermediate

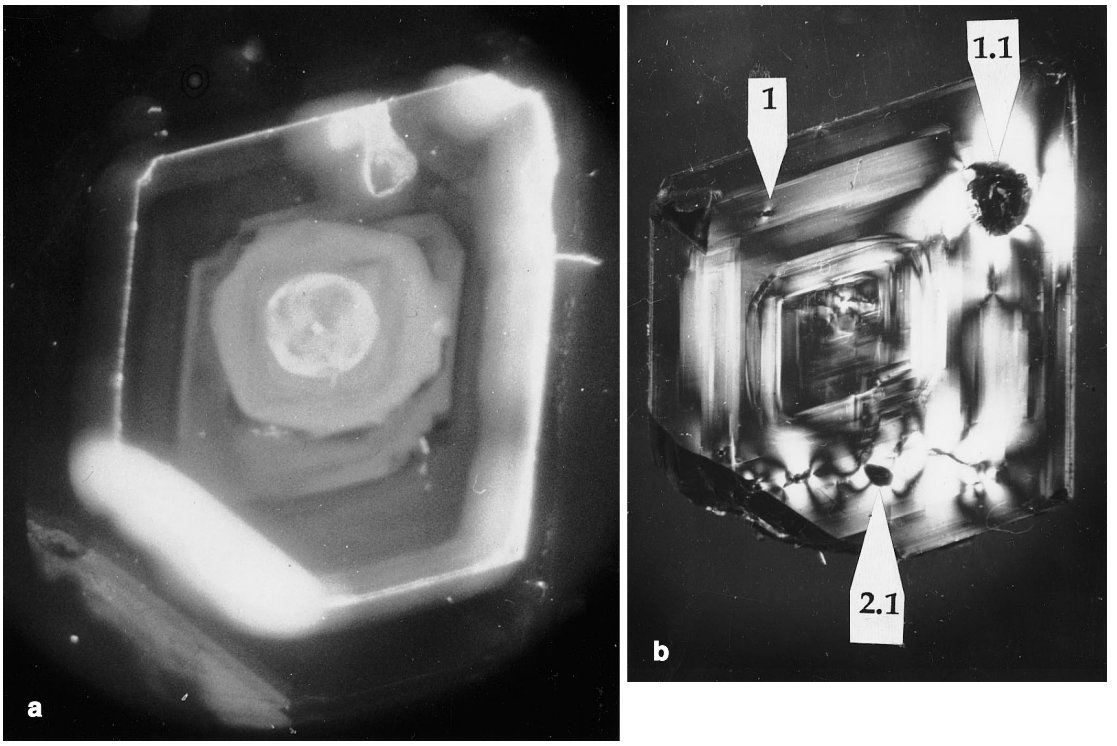


**Fig. 6** Photoluminescence (**a**) and birefringence (**b**) images of diamond plate 1153, showing location of SDIs, and evolution of the diamond morphology from cube to rounded form to octahedron. Width of crystal 4 mm

zone, one sulfide inclusions coexists with omphacite. Tellurium was detected only in one of the core-zone inclusions; on average, Se is higher in the inclusions from the intermediate and peripheral zones, but Mo shows no consistent pattern.

*Diamond 4173 (eclogitic paragenesis)*

This stone consists of two growth zones, a cubo-octahedral central zone and an octahedral outer zone. Both luminesce blue, but with different intensity. In the outer zone, two separate inclusions of omphacite and coesite coexist with the sulfides. There is no significant difference between the two sulfide inclusions analyzed.

As a generalization it appears that SDIs from diamonds with simple internal structures, consistent with continuous single-stage growth, show little variation in chemistry, whereas those with complex internal structures contain SDIs with a relatively wide range in trace-element composition. A similar observation linking internal structural complexity and variable inclusion chemistry has been made for silicate and oxide inclusions (Bulanova 1995).

## Discussion

Eclogitic versus peridotitic parageneses

There are major differences between the sulfides trapped in eclogitic diamonds and those in peridotitic diamonds. The eclogitic SDIs are distinctly lower in Ni, Cu and Te; the ranges of the two parageneses in Se, As and Mo overlap, but the highest values are found in the peridotitic SDIs. The peridotitic SDIs also show a very wide variation in Se and Mo contents in comparison with the eclogitic SDIs. Figure 1 suggests that peridotitic SDIs can be divided into two groups with high and low contents of Se and Mo. The PGEs have been found at detectable levels only in the peridotitic SDIs.

The compositional similarities and differences between the two suites mirror in general those between magmatic sulfide deposits associated with ultramafic and mafic magmas. Magmatic sulfide deposits of all types typically have S/Se ratios of 2000–10 000 (compared to >20 000 for sediment-hosted deposits; Naldrett 1981). Both types of SDI show a pronounced peak in Se contents near 50 ppm, corresponding to S/Se ≈7000. Higher values from 100–150 ppm, correspond to S/Se ratios of ≈2500–3500.

The eclogitic SDIs have Ni/Cu ratios within the range of many gabbro-related magmatic sulfide deposits, including Sudbury (Naldrett 1981). The peridotitic SDI have Ni/Cu ratios higher than most crustal sulfide deposits, but similar values are found in deposits associated with some Archean komatiites. The Zn and Pb contents of komatiite-related sulfides typically are low

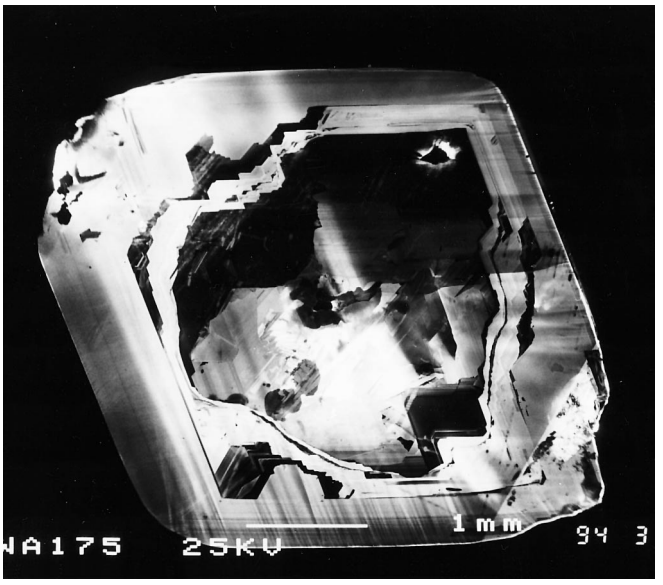


**Fig. 7** Cathodoluminescence image of sawn plate of diamond 1607, showing internal zonation. Several of the sulfide inclusions are visible as dark spots, especially in the outer zone. Width of crystal 3.6 mm

(<200 ppm Zn, <15 ppm Pb) and both elements are similarly low in the peridotitic SDIs. Higher values (100–>2000 ppm Zn, 14–>200 ppm Pb) are characteristic of gabbro-related magmatic sulfides, and similar ranges are seen in the eclogitic SDIs that are inferred to be pristine.

Copper,Se,Te, As and Mo are all elements typical of crustal sulfide deposits. The lower abundances of these elements in the mafic (eclogitic SDIs), and their generally higher abundances in the sulfides from the ultramafic paragenesis, therefore were unexpected. The lower abundances of the chalcophile elements (and PGEs) in the eclogitic sulfides suggest that the eclogites may be cumulates, or residues, from which chalcophile elements have been removed in a previous magmatic or metasomatic episode. The fluids from which the eclogitic diamonds later grew therefore had low chalcophile-element contents, even though they must have been sulfur saturated.

## MSS-sulfide melt fractionation?

The temperature range previously established for silicate and oxide inclusions in diamonds from Siberia (Griffin et al. 1993) spans the range of coexistence of sulfide melts and MSS crystals. This suggests that sulfides might be trapped either as droplets of immiscible sulfide melt, such as those described from many silicate megacrysts in basalts (see Andersen et al., 1987, for review), or as crystals of MSS crystallized from such melts. The presence of both types of sulfide could help to explain some of the large ranges in element concentrations seen in these inclusions.

The analysis of compositional differentiation in magmatic sulfide deposits, combined with empirical estimates of element partitioning between sulfide melts and MSS, has produced successful models of such ore deposits based on fractional-crystallization models (e.g., Hawley 1962; Naldrett et al. 1994; Zientek et al. 1994). Experimental studies of MSS-melt partitioning are now providing more precise data, and elucidating the effects of melt composition and temperature on element distribution between sulfide melt and MSS (Barnes et al. 1995; Li et al. 1995).

These empirical and experimental studies suggest that during fractional crystallization, Os, Ir, Ru and Rh are concentrated in MSS, while elements such as Cu, Se, Te, Pt and Pd remain in the residual liquid. The $D_{Ni}^{(MSS/melt)}$ is generally <1, with most experimental values in the 1000–1100° C range lying between 0.3 and 0.8, so that Ni also is concentrated in melt, though weakly. Fractional crystallization from immiscible sulfide melts therefore would be expected to produce MSS crystals with low Ni, Cu and high Ir/Pd, while the residual melts would be enriched in Ni, Cu, Se, Te and Pd. Some of the SDI data fit this general pattern. Within the eclogitic SDI these are essentially two groups, one with low Ni and Cu (within which Ni and Cu are positively correlated), the other with higher Ni and Cu. The highest Se and Mo contents are found among the sulfides with Cu>1%; these may represent trapped melts, while the low-Ni,Cu group could then represent the corresponding MSS.

Among the peridotitic SDIs, we find a low-Ni population (12–17% Ni) with very low Cu, and a higher-Ni group with generally higher Cu. Among the peridotitic inclusions with Cu>3% are a number with high Se, Te, Mo and Pd, which may represent trapped melts; most of the SDIs that contain Pd or Pd+Rh, as the only detectable PGEs, fall into this group.

The unusually PGE rich inclusions in diamond 3648 have mantle-normalized Os,Ir-enriched PGE patterns that set them apart from other mantle-derived sulfides, most of which have been interpreted as representing sulfide melts (Fig. 8). However, the overall shape of this pattern corresponds to that predicted for MSS crystallizing from sulfide liquids (Fig. 9) using the partition coefficients of Barnes et al. (1996) and Li et al. (1996). This similarity of pattern strongly suggests that these particular SDIs were trapped as MSS crystals, rather than as sulfide melts. The quantitative difference between the predicted pattern and the observed ones suggests either that there is an overall pressure effect on PGE partition coefficients, or that the sulfide melt from which these MSS crystals formed had PGE contents ca 10× those observed in sulfides from spinel lherzolite xenoliths. The latter interpretation seems more probable, especially since the diamonds and the spinel lherzolites come from quite different depths and tectonic environments.

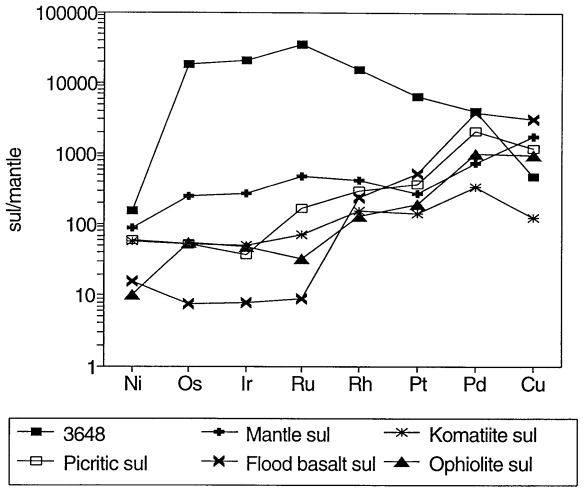


**Fig. 8** Comparison of mantle-normalized metal patterns of SDIs from core of diamond 3648 (Fig. 4) and various mantle-derived sulfides, believed to be immiscible melts in mafic to ultramafic rocks. "Mantle sulfides" are from Pattou et al. (1996). Other data from Barnes et al. (1988)

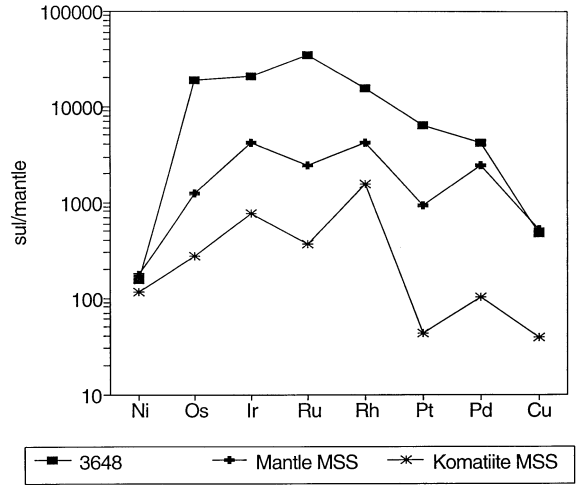


**Fig. 9** Comparison of mantle-normalized metal patterns of SDI from core of diamond 3648 (Fig. 4) with model MSS in equilibrium with mantle sulfide (liquid) and komatiite sulfide liquid

## Ni content of sulfides

The broad differences in Ni content between eclogitic and peridotitic sulfides are easily understood in terms of the general differences between the Ni contents of mafic and ultramafic environments, and partitioning between sulfide and coexisting silicates. The peridotitic sulfides probably equilibrated with large volumes of mantle olivine, which typically contains 2500–3000 ppm Ni (Griffin et al. 1989; Ryan et al. 1996), and controls the Ni content of the peridotitic environment. The eclogitic SDIs probably equilibrated with eclogitic garnet and clinopyroxene, which typically contain a few hundred ppm Ni (O'Reilly and Griffin 1995), and define the lower Ni content of the eclogitic environment. Sulfide melts in equilibrium with an eclogitic bulk composition therefore will have lower Ni than those in ultramafic environments.

The SDIs known or believed to be from the peridotitic paragenesis range from 22% to 35% Ni. Within single diamonds, ranges of 24–31% have been observed; this may be an artifact of sectioning heterogeneous inclusions, but the agreement between EMP and PMP values in most cases suggests the variation is real, and reflects changes in the environment in which the diamond grew.

Fleet et al. (1977) and Fleet and MacRae (1987, 1988) studied the controls on Ni/Fe exchange between olivine and MSS. The distribution coefficient defined by these experiments is essentially constant over the $T$ range 900–1400° C and a wide range of $f_{O_2}$ and $f_{S_2}$, including compositions controlled by the IW (iron-wustite) buffer. Given a range in peridotitic olivine from $Fo_{88}$-$Fo_{94}$ and 2500–3500 ppm Ni, the coexisting MSS will range from 30–55 mol% NiS (25–35 wt% Ni). Equilibrium with the average mantle olivine should produce a MSS with $\approx$50 mol% NiS ($\approx$32 wt% Ni). This range in composition corresponds approximately to one of the Ni populations defined above, with 22–36.5% Ni and a median value of 26 wt% ($n$=19); the difference from the experimentally predicted mean probably is within the respective experimental and analytical errors, and also may be influenced by the Cu content of the system. However, it also may be real, and indicate that many of the SDIs are in fact MSS that crystallized from sulfide melts in equilibrium with mantle olivine. As noted above, $D_{Ni}^{(MSS/melt)}$ is generally $<1$ in the relevant $T$ interval (Barnes et al. 1995). In diamond 3648, inclusion 2.1 coexists with an olivine $Fo_{93}$, which has not been analyzed by proton probe but probably (by analogy with many other analyses) contains ca 3000 ppm Ni; the sulfide contains 31% Ni, as predicted by these experiments. Our data therefore suggest that these peridotitic SDIs (either as sulfide melts or as crystals forming from those melts) were approximately in equilibrium with mantle olivine at the time of their trapping in the diamonds.

Similar experimental work by Boctor (1981) and Boctor and Yoder (1983) measured Ni distribution between olivine and sulfide melt, under conditions with controlled oxygen and sulfur fugacity and at $T$=1300–1400° C. These experiments yielded distribution coefficients roughly half those of Fleet et al. (1977); it would not be possible to produce Ni contents like those of the present peridotitic SDIs by equilibrium between sulfide melt and mantle olivine using these distribution coefficients. The problem is exacerbated if $D_{Ni}^{(MSS/Melt)}$ is $<1$. This contradiction suggests that the coexistence of the high-Ni SDIs with typical mantle olivine (which is the next most common inclusion in diamonds worldwide) reflects a strong $T$ effect on $K_D$, so that the low $K_D$ values observed by Boctor (1981) and Boctor and Yoder (1983) at 1300–1400° C increase to values similar to those reported by Fleet et al. (1977) and Fleet and MacRae (1987, 1988) as $T$ drops to 1000–1100° C.

The inclusions with ≈12–19% Ni may represent a third diamond paragenesis, derived from magnesian pyroxenites ± garnet; none are from diamonds that contained olivine inclusions, while one is from an omphacite-bearing stone. This diamond paragenesis was recognized by Griffin et al. (1992) on the basis of garnet inclusions with abnormally low Ni and Cr contents, and elevated Fe contents. The SDIs in such diamonds might have equilibrated with relatively low Ni pyroxene in olivine-free rocks. Alternatively, some lower-Ni SDI may have been modified by post-crystallization processes, perhaps by cracks to a paleosurface. Further work to correlate sulfide compositions with coexisting silicates will be necessary before this paragenesis can be recognized solely on the basis of sulfide chemistry.

## Diamond growth

The complex diamond 3648 shows at least three distinct zones; the SDIs in these zones show similar S-isotope compositions but different Pb-isotope compositions. Rudnick et al. (1992) have interpreted the Pb-isotope data as showing a three-stage growth history: (1) formation of the diamond core in a peridotitic environment at about 2 Ga; (2) formation of the intermediate zone in a high-U/Pb environment similar to that of some eclogitic diamonds; (3) formation of the outer zone during a shortly before eruption of the host kimberlite. The cathodoluminescence studies of this diamond (Bulanova 1995; Taylor et al. 1995) and the trace-element data on the SDIs added further constraints to this history. The intermediate-zone SDI shows the same high Mo, Te, PGE and Ni contents as the core-zone SDIs, indicating that it formed in a peridotitic, rather than an eclogitic, environment. The Se and Mo levels of the outer-zone SDIs are not diagnostic of either the eclogitic or the peridotitic environment, but their PGE contents are significantly higher than those of any clearly eclogitic inclusions.

The PGE contents of the low-Pb SDI decrease rimward, but are high in all zones relative to most other diamonds we have analyzed. There is a continuous change from core to rim, with Pd, Rh and Ru decreasing relative to Ir and Os as total PGEs decrease, while Ni and Cu contents stay essentially constant at 12–15 times chondrites (Ni) and 75–95 times chondrites (Cu). This variation is consistent with a simple (closed-system?) fractionation during the growth of the diamond, rather than any marked change in the chemical environment. We argued above that the SDIs in diamond 3648 probably were trapped as MSS crystallizing from a sulfide melt. Continuous fractional crystallization of MSS would deplete the melt in Os and Ir relative to Ru and Rh, and this would be reflected in a drop in Ir/Rh and in Ir/Cu, in successive MSS compositions. Neither effect is observed. The depletion of Rh and Ru relative to Os and Ir, while Cu and Ni remain essentially constant, may require fractionation of a third phase enriched in Rh and Ru. This phase may resemble the unusual SDI 5/5, which contains Ru and Rh at levels 10× those of the SDIs in diamond 3648, but no other PGEs, while Ni and Cu concentrations are similar to the SDIs in diamond 3648.

The main difference between the SDIs of the outer zone and those of the core and intermediate zones is in the high Pb content of most of the outer-zone SDIs. This suggests that Pb leaked into some outer-zone SDIs via cracks to the surface, without affecting the abundance of the other elements. This may have occurred during the kimberlite event, but in this case the inclusions are not strictly syngenetic, and their Pb-isotopes do not necessarily reflect diamond growth during the kimberlite stage, as suggested by Rudnick et al. (1992). The radiogenic Pb-isotope composition of the intermediate-zone inclusion (no. 7.3; Fig. 5) suggests that it was opened to a fluid via a crack to the paleosurface of the crystal, during resorption and regrowth of the diamond, as described by Taylor et al. (1995). It has a low Pb content, and its isotopic composition could have been easily modified, apparently without affecting the trace-element content of S-isotope composition of the sulfide.

We therefore suggest that the growth of this diamond took place in a peridotitic environment, in several stages. A change in physical conditions caused resorption of the diamond between the intermediate and rim stages, but the diamond apparently continued to grow from the same chemical environment after this resorption had taken place. Some of the inclusions in the intermediate outer part of the diamond were open (via fractures) to an environment with a high time-integrated U/Pb ratio after their formation, but only their Zn and Pb contents (and Pb isotopic compositions) were significantly affected. The diamond apparently was able to anneal at least some of these fractures prior to eruption (Taylor et al. 1995).

Naldrett (1969) showed that Fe-S melts can dissolve substantial amounts of oxygen, and this typically appears as exsolved magnetite in quenched magmatic sulfides, such as those in basalts. In the SDIs studied here magnetite is rare, and most cases are in inclusions that show evidence (high Pb and/or Zn) of interaction with the external environment via cracks in the diamond. The general absence of oxides even in the high-Cu SDIs that might be interpreted as trapped melts may reflect the extremely reducing conditions of diamond growth (IW buffer; Bulanova 1995), and also may indicate that the solubility of oxygen in Fe−Ni−S melts is significantly lower at P≥40 kbar than under low-*P* conditions.

## Primitive mantle sulfides?

The high levels of PGEs recorded in several peridotitic SDIs appear to reside in the MSS structure; examination of these inclusions by SEM has failed to reveal the presence of discrete PGE-bearing minerals. This does not rule out the presence of discrete PGE phases below the surface of each inclusion, where they would still be analyzed by the proton beam. However, if this is the case, the

rimward decrease in total PGE in the SDIs of diamond 3648, and the associated changes in the PGE patterns, would have to reflect changes in the abundance and composition of such phases. This would still suggest that the PGE abundances are a primary feature of the sulfide melt, with the PGE phases either nucleating within the melt or exsolving from the MSS during cooling. The high PGE levels are found in the sulfides with intermediate Ni contents (25–30%) and Cu contents of 1–2%. They are not found in the high-Ni (>30%), low-Cu SDIs. These data suggest that the PGE-rich SDIs may represent a distinct class of primitive lithospheric sulfides. They also may be restricted to a group of diamonds with unusually complex internal structures though the present data are very limited. The highest PGE levels are found in diamond 3648, which is unusual in having inclusions of wustite. Harte and Harris (1994) have suggested that diamonds with the inclusion assemblage magnesiowustite +enstatite+garnet are derived from sublithospheric depths. By analogy, the unusual inclusion assemblage, internal structure and sulfide chemistry of this diamond may suggest that it is derived from greater depth than most of the other diamonds studied here, even though the wustite in this case is not magnesian.

Fleet and Stone (1991) and Fleet et al. (1991) have determined the partitioning of PGEs between Fe−Ni−PGE alloys, sulfide melts and MSS at one atmosphere, and to 11 GPa, respectively. Barnes et al. (1996) and Li et al. (1996) have carried out more detailed studies of partitioning between MSS and sulfide melts. Comparison with our data suggests that a range of parageneses may be represented. In general Os, Ir and Pt tend to be concentrated in alloy phases, whereas Pd is enriched in the coexisting sulfide melt. Ruthenium, and to a lesser extent Rh, are preferentially enriched in troilite coexisting with sulfide melts. Inclusions such as 5/5, strongly enriched in Ru and Rh but depleted in the other PGEs may represent troilite that coexisted with a sulfide liquid, or may contain inclusions of an unknown Ru−Rh phase. Sulfides with Os−Ir enrichment, such as those in diamond 3648, cannot have coexisted with an alloy phase, and probably represent MSS crystallized from a sulfide liquid. Conversely, inclusions such as 9/14 which contain Pd but are depleted in the other PGEs may represent the sulfide liquid residual after fractional crystallization of a MSS phase.

Upper mantle xenoliths commonly have PGE patterns that are flat (unfractionated relative to chondrites; Crockett 1979), whereas crustal sulfides typically are enriched in Pt and Pd. This distribution, and the Os−Ir enrichment in the chromitites and dunites of ophiolite complexes, has led to the suggestion that alloy phases are residual in the mantle during melting events that produce mafic magmas (Amosse et al. 1987). However, the SDIs in diamond 3648 show that some mantle sulfides also can concentrate Os and Ir, and that alloy phases are not necessary to explain the crust/mantle fraction of the PGEs.

Hamlyn et al. (1985) explained the association of crustal magmatic PGE deposits with low-Ti magmas by proposing a two-stage melting process. In the first stage, corresponding to the extraction of basaltic melts, relatively low degrees of partial melting allowed retention of very small volumes of sulfide in the residual mantle. Magma/sulfide partitioning would tend to remove base metals and Se, concentrating PGEs in the mantle sulfide. This also would lead to enrichment of the Os, Ir end of the PGE group. The second stage of the process, involving high degrees of partial melting, would leave no sulfide in the residue, and would produce low-Ti magmas with low S contents but relatively high PGE levels. In this model, peridotitic SDIs, and especially ones like those in diamond 3648, might conceivably represent residual sulfides from the first stage of melting. However, these "residual" sulfides also should be depleted in elements such as Cu, Se and Te, which would be partitioned into the melt (Barnes et al. 1995). Since they are not, it appears improbable that many of the peridotitic SDI are residual from basalt extraction, and more likely that they are primitive, if not primordial, mantle sulfides.

**Acknowledgements** We thank Tin Tin Win for essential assistance with the data collection. M. Tredox contributed many useful discussions on the PGE chemistry of sulfides, and the paper was improved by a thoughtful review from Steve Barnes. This is publication no. 23 from the Key Centre for Geochemical Evolution and Metallogeny of Continents (GEMOC).

## References

Amosse J, Allibert M, Fischer W, Piboule M (1987) Étude de l'influence des fugacités d'oxygène et de soufre sur la differenciation des platinoides des magmas ultramafiques. Resultats preliminaires. CR Acad Sci 304(ii):1183–1185

Andersen T, Griffin WL, O'Reilly SY (1987) Primary sulfide melt inclusions in mantle-derived megacrysts and pyroxenites. Lithos 20: 279–294

Barnes S-J, Boyd R, Korneliussen A, Nilsson L-P, Often M, Pedersen RB, Robins B (1988) The use of mantle normalization and metal ratios in discriminating between the effects of partial melting, crystal fractionation and sulphide segregation on platinum-group elements, gold, nickel and copper: examples from Norway. In: Prichard HM, Potts PJ, Bowles JFW, Cribb SJ (eds) Geoplatinum-87. Elsevier, London, pp 113–143

Barnes SJ, Makovicky E, Karup-Moller S, Makovicky M, Rose-Hansen J (1996) Parition coefficients for Ni, Cu, Pd, Pt, Rh and Ir between monosulfide solid solution and sulfide liquid and the formation of compositionally zoned Ni−Cu sulfide bodies by fractional crystallization of sulfide liquid. Can J Earth Sci (in press)

Boctor NZ (1981) Partitioning of nickel between olivine and iron sulfide melts. Carnegie Inst Washington Yearb 80: 356–359

Boctor NZ, Yoder HS (1983) Partitioning of nickel between olivine and iron monosulfide melts. Carnegie Inst Washington Yearb 82: 275–277

Bulanova GP (1996) The formation of diamond. In: Griffin WL (ed) Diamond exploration: into the 21st century. J Geochem Explor 53: 1–23

Bulanova GP, Spetsius ZV, Leskova NV (1990) Sulfides in diamonds and mantle xenoliths from kimberlite pipes of Yakutia. Nauka, Novosibirsk

Craig JR, Kullerud G (1969) Phase relations in the Cu−Fe−Ni−S system and their application to magmatic ore deposits. Econ Geol Monogr 4: 344–358

Crockett JH (1979) Platinum-group elements in mafic and ultramafic rocks: a survey. Can Mineral 17: 391–402

Davis GL (1977) The ages and uranium contents of zircons from kimberlites and associated rocks. Carnegie Inst Washington Yearb 76: 631–635

Eldridge CS, Compston W, Williams IS, Harris JW, Bristow JW (1991) Isotope evidence for the involvement of recycled sediments in diamond formation. Nature 353: 649–653

Erasmus CS, Sellschop JPF, Bibby DM, Fesq HW, Kable EJD, Keddy RJ, Hawkins DM, Mingay DW, Rasmussen SE, Renan MJ, Watterson JIW (1977) Natural diamonds – major, minor and trace impurities in relation to source and physical properties. J Radioanal Chem 38: 133–146

Fleet ME, MacRae ND (1987) Partition of Ni between olivine and sulphide: the effect of temperature $f_{O_2}$ and $f_{S_2}$. Contrib Mineral Petrol 95: 75–81

Fleet ME, MacRae ND (1988) Partition of nickel between olivine and sulfide: equilibria with sulfide-oxide liquids. Contrib Mineral Petrol 100: 462–469

Fleet ME, MacRae ND, Herzberg CT (1977) Partition of nickel between olivine and sulfide: a test for immiscible liquids. Contrib Mineral Petrol 65: 191–197

Fleet ME, Stone WE (1991) Partitioning of platinum-group elements in the Fe−Ni−S system and their fractionation in nature. Geochim Cosmochim Acta 55: 245–253

Fleet ME, Tronnes RG, Stone WE (1991) Partitioning of platinum group elements in the Fe−O−S system to 11 GPa and their fractionation in the mantle and meteorites. J Geophys Res 96: 21949–21958

Griffin WL, Cousens DR, Ryan CG, Sie SH, Suter GF (1989) Ni in chrome pyprope garnets: a new geothermometer. Contrib Mineral Petrol 103: 199–202

Griffin WL, Gurney JJ, Ryan CG (1992) Variations in trapping temperatures and trace elements in peridotite-suite inclusions from African diamonds: evidence for two inclusion suites, and implications for lithosphere stratigraphy. Contrib Minereal Petrol 110: 1–15

Griffin WL, Sobolev NV, Ryan CG, Pokhilenko NP, Win TT, Yefimov Y (1993) Trace elements in garnets and chromites: diamond formation in the Siberian lithosphere. Lithos 29: 235–256

Gurney JJ, Harris JW, Rickard RS (1979) Silicate and oxide inclusions in diamonds from the Finish kimberlite pipe. In: Boyd FR, Meyer HOA (eds) kimberlites, diatremes and diamonds. Am Geophys Union, Washington, pp 1–15

Hamlyn PR, Keays RR, Cameron WE, Crawford AJ, Waldron HM (1985) Precious metals in magnesian low-Ti lavas: implications for metallogenesis and sulfur saturation in primary magmas. Geochim Cosmochin Acta 49: 1797–1811

Harte B, Harris JW (1994) Pyrope-almandine garnet in lower mantle mineral parageneses from Sao Luiz, Brazil. EOS Trans Am Geophys Union 75: 192

Harris JW, Gurney JJ (1979) Inclusions in diamond. In: Field JE (ed) The properties of diamond. Academic Press, London, pp 555–591

Hawley JE (1962) The Sudbury ores: their mineralogy and origin. Mineral Assoc Can, Univ Toronto Press, Toronto

Kaminsky FV, Franteson YeV, Khvostova VP (1974) First information on Platnium Metals (Pt, Pd, Rh, Ir, Ru, Os) in kimberlitic rocks. Dokl Acad Sci USSR Earth Sci Sect 219: 190–193

Loraud J-P (1989) Abundance and distribution of Cu−Fe−Ni sulfides, sulfur, copper and platinum-group elements in the orogenic-type spinel lherzolite massif of Ariège. Earth Planet Sci Lett 93: 50–64

Li C, Naldrett AJ, Rucklidge JN, Kilius LR (1993) Concentrations of platinum-group elements and gold in sulfides from the Strathcona deposit, Sudbury, Ontario. Can Mineral 30: 523–531

Li C, Barnes S-J, Makovicky E, Rose-Hansen JR, Makovicky M (1996) Partitioning of Ni, Cu, Ir, Rh, Pt and Pd between monosulfide solid solution and sulfide liquid: effects of composition and temperature. Geochim Cosmochin Acta (in press)

McDonald I, Harris JW, Vaughan DJ (1995) Noble metals in sulphide inclusions from diamonds (unpublished abstract). Diamond Conf, London

Mitchell RH, Keays RR (1981) Abundance of gold, palladium and iridium in some spinel and garnet lherzolites: implications for the nature and origin of precious metal-rich intergranular components in the upper mantle. Geochim Cosmochim Acta 45: 2425–2442

Morgan JW, Wandless GA, Petrie RK, Irving AJ (1981) Composition of the Earth's upper mantle. 1. Siderophile trace elements in ultramafic nodules. Tectonophysics 75: 47–67

Naldrett A (1969) A portion of the system Fe−S−O between 900° C and 1080° C and its application to sulfid ore magmas. J Petrol 10: 171–201

Naldrett AJ, Duke JM (1980) Platinum metals in magmatic sulfide ores. Science 208: 1417–1424

Naldrett AJ (1981) Nickel sulfide deposits: classification, composition and genesis. Econ Geol 75th Anniv Vol: 628–685

Naldrett AJ, Asif M, Gorbachev NS, Kunihov VYe, Stekin AI, Fedorenko VA, Lightfoot PC (1994) The composition of the Ni−Cu ores of the Noril'sk region. In: Lightfoot PC, Naldrett AJ (eds) The Sudbury-Noril'sk Symposium. Ont Geol Surv Spec Publ 5, pp 357–372

Pattou L, Lorand JP, Gros M (1996) Non-chondritic platinum-group element ratios in the Earth's mantle. Nature (in press)

O'Reilly SY, Griffin WL (1995) Trace element partitioning between garnet and clinopyroxene in mantle-derived pyroxenites and eclogites: *P-T-X* controls. Chem Geol 121: 105–130

Pactune AD, Hulbert LJ, Harris DC (1990) Partitioning of the platinum-group and other trace elements in sulfides from the Bushveld complex and Canadian occurrences of nickel-copper sulfides. Can Mineral 28: 475–488

Page NJ, Talkington RW (1984) Palladium, platinum, rhodium, ruthenium and iridium in peridotites and chromites from ophiolite complexes in Newfoundland. Can Mineral 22: 137–148

Page NJ, Singer DA, Moring BC, Carlson CA, McDade JM, Wilson SA (1986) Platinum-group element resources in podiform chromites from California and Oregon. Econ Geol 81: 1261–1271

Paul D, Crocket JH, Nixon PH (1979) Abundances of Pd, Ir and Au in kimberlites and associated nodules. Proc 2nd Int Kimberlite Conf, vol 1. Am Geophys Union, Washington, DC, 272–279

Rivers ML, Dawson JB, Smith JV (1990) Trace element studies of sulfides from the upper mantle. EOS Trans Am Geophys Union 71: 524

Rudnick RL, Eldridge CS, Bulanova GP (1992) Diamond growth history from in situ measurement of Pb and S isotopic compositions of sulfide inclusions. Geology 21: 13–16

Ryan CG, Cousens DR, Sie SH, Griffin WL, Suter GF (1990) Quantitative PIXE micronalaysis of geological material using the CSIRO proton microprobe. Nucl Instrum Methods B47: 55–71

Ryan CG, Griffin WL, Pearson NJ (1996) Garnet geotherms: a technique for derivation of *P-T* data from Cr-pyrope garnets. J Geophys Res 101: 5611–5625

Stockman HW, Hlava PF (1984) Platinum-group minerals in alpine chromitites from southwestern Oregon. Econ Geol 79: 491–508

Taylor WR, Bulanova G, Milledge HJ (1995) Quantitative nitrogen aggregation study of some Yakutian diamonds: constraints on the growth, thermal and deformation history of peridotitic and eclogitic diamonds (abstract). In: Abst 6th Int Kimberlite Conf Novosibirsk, pp 608–610

Yefimova ES, Sobolev NV, Pospelova LN (1983) Inclusions of sulfides in diamonds and their paragenesis (in Russian). Zap Vses Mineral va CXII: 300–309

Zientek MlL, Likhachev AP, Kunilov VE, Barnes S-J, Meier A-L, Carlson RR, Briggs PH, Fries TL, Adrian BM (1994) Cumulus processes and the composition of magmatic ore deposits: examples from the Talnakh district, Russia. In: Lightfoot PC, Naldrett AJ (eds) The Sudbury-Noril'sk Symposium. Ont Geol Surv Spec Publ 5, pp 357–372